

Electron spin resonance and structure of magnetically inequivalent chains in $\text{CuCl}_2 \cdot 2\text{NC}_5\text{H}_5$ †

R. C. Hughes, B. Morosin, and Peter M. Richards
Sandia Laboratories, Albuquerque, New Mexico 87115

W. Duffy, Jr.

Department of Physics, University of Santa Clara, Santa Clara, California 95053

(Received 4 September 1974)

Interchain exchange coupling J' between magnetically inequivalent chains has been studied in the quasi-one-dimensional (1d) salt dichlorobis(pyridine)copper(II) ($\text{CuCl}_2 \cdot 2\text{NC}_5\text{H}_5$, referred to as CPC). Except along symmetry directions, the two types of chains have different g factors, and therefore two separate ESR lines would be seen in the absence of J' . The coupling J' merges the lines, but the width of the single observed line is proportional to the square of the microwave frequency. From the known splitting in the absence of J' , determined from previous studies of the crystal g tensor, and measurements at 10.9 and at 35 GHz, we deduce $|J'/J| = 1.2 \times 10^{-2}$, where J is the strong intrachain interaction. Previous theories of ESR in quasi-1d systems were used to relate the linewidth to J' . In the course of the work a refined determination of the structure has been made and the various possible interchain exchange paths have been elucidated. In regard to the latter, it is noted that since there are in general three different interchain exchange constants which combine differently in their effects on the linewidth and on the ordering temperature T_N , direct comparison cannot be made between the effective J' reported here and that inferred from T_N .

I. INTRODUCTION

There is now a fairly large number of inorganic and organic crystals made of paramagnetic entities which display the magnetic characteristics of one-dimensional (1d) chains of strongly exchange-coupled spins.^{1,2} An important quantity in the understanding of the magnetism in these quasi-1d systems is the degree of one-dimensionality, i. e., the ratio of the interchain exchange to the intrachain exchange, J'/J . In this paper we report a method for determining J' which has not been used before in an inorganic paramagnetic-ion linear-chain salt.³ It is applicable in systems in which the chains are magnetically inequivalent, and is applied here to the salt dichlorobis(pyridine)copper(II) ($\text{CuCl}_2 \cdot 2\text{NC}_5\text{H}_5$, hereafter referred to as CPC) by measuring the frequency dependence of the EPR linewidth. The magnetic properties of CPC have been studied extensively,^{4,5} and it is one of the best-documented quasi-1d systems. In particular, in a paper⁵ referred to as I, the average g tensor has been measured and interpreted in terms of the separate g 's for the inequivalent chains.

If the J' were very small, then one would see two ESR lines for many angles of the applied field to the crystal, and the difference in resonance field between the lines would be proportional to the microwave frequency employed, owing to the different effective g factors of the chains. The exchange between chains, J' , tends to average the two lines and in the case of CPC is strong enough so that only one line is observed, even at the highest Larmor

frequency used (35 GHz) and the angle of maximum splitting. However, the linewidths are very frequency dependent, since the width of the averaged line is roughly $(\text{splitting})^2/(\text{exchange rate})$. Thus comparison of the linewidth at X band (10.9 GHz) and Q band (35 GHz) is sufficient to make a determination of J' .

A rough determination of J'/J can be made even if the chains are not magnetically inequivalent by using the frequency dependence of the linewidth due to anisotropic dipolar interactions between chains to determine the Fourier components of the spin correlation function, as was recently done^{6,7} for the salt $\text{Cu}(\text{NH}_3)_4\text{PtCl}_4$.

A linear antiferromagnetically coupled chain has a magnetic susceptibility which peaks at $kT \sim J$ and decreases isotropically below that temperature due to short-range magnetic order along the chain. In many of the inorganic salts long-range magnetic ordering sets in at some lower temperature (T_N), which reflects the exchange between chains, and thus a J' can be estimated⁸ from T_N . Care must be taken, however, because in some crystals, CPC included, there may be more than one interchain exchange constant J' , and the constants can combine differently in their contributions to T_N and to the frequency-dependent linewidth. A particularly simple example is that exchange between equivalent chains will affect T_N but not this linewidth. In CPC the situation is somewhat more complex, as discussed in Sec. II B.

If J'/J is very small, the spin excitations remain on a single chain for a long time and the EPR line

shape will no longer be Lorentzian, but will lie somewhere between a Gaussian and a Lorentzian shape, reflecting the diffusive behavior of the spins along the chain.⁹ If the line shape is found to be Lorentzian at all angles to the chain as in CPC, then the theoretical treatment of Hennessy *et al.*¹⁰ predicts that J'/J will be greater than 10^{-3} , which is consistent with the $J'/J = 1.2 \times 10^{-2}$ reported here for CPC.

J' may also be determined from careful neutron-scattering measurements of the spin-wave spectrum in the ordered phase, as has been done¹¹ for $\text{CsMnCl}_3 \cdot 2\text{H}_2\text{O}$. However, energy resolution is generally not sufficient to measure the small dispersion perpendicular to the chain.

Ideally one would like to have a system for which a single J' could be inferred from all the above-mentioned methods, so that the various theories could be checked for consistency. In principle this could be accomplished in a crystal which had magnetically inequivalent chains, a simple ordering structure characterized by one interchain exchange constant only—and that between inequivalent chains, and a value of J'/J small enough to observe non-Lorentzian lines but large enough to be amenable to neutron scattering. CPC, unfortunately, fulfills only the first requirement, but it is the first linear-chain compound which displays long-range order at low temperature in which the effects of inequivalent chains have been tested for J' . We are unaware of any compound which has all the desired features.

The paper is organized as follows. New data on the structure are presented in Sec. II A, with particular emphasis on how they relate to principal axes for the g tensors. Section II B discusses the possible interchain superexchange interactions in view of the structure. Experimental details are given in Sec. III, and results for the linewidth are presented in Sec. IV. A theory which relates the effective exchange rate to the interchain coupling is derived in Sec. V. Sections VI and VII contain a discussion and a summary and conclusions, respectively.

II. STRUCTURAL DETAILS

A. Atomic positions

The crystal structure of CPC was initially reported by Dunitz.¹² As part of a continuing study on structural properties of linear-chain compounds, we have refined by least-squares method the structural parameters employing 1270 different hkl intensities.

CPC crystallizes in space group $P2_1/n$ in a cell of dimensions $a = 16.967 \text{ \AA}$, $b = 8.56 \text{ \AA}$, $c = 3.848 \text{ \AA}$, and $\beta = 91.98^\circ$. The Cu^{2+} ion is surrounded by four closer neighbors consisting of two Cl_s ions at 2.298

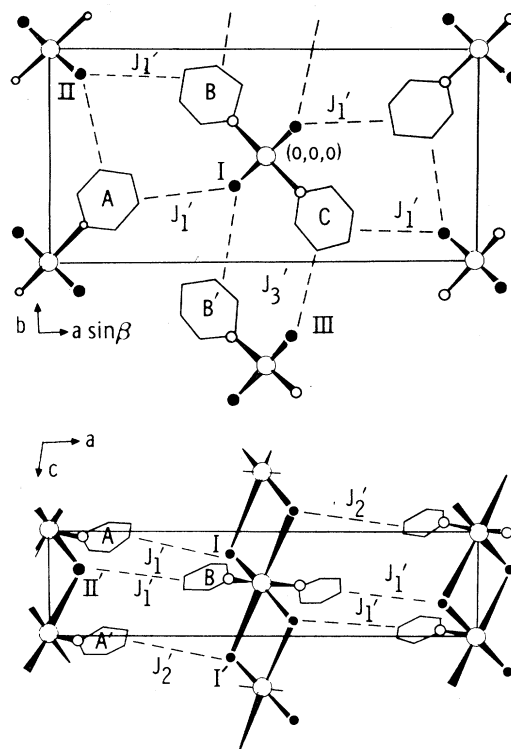


FIG. 1. Schematic drawing of the structure of CPC. The top view is parallel to the linear chains found in CPC; the bottom view along the b axis (the 91.98° angle between a and c directions on the label only has been purposely exaggerated). The Cu^{2+} environment consists of four closer atoms consisting of two Cl_s at 2.298 \AA and two nitrogen atoms at 2.004 \AA and two more distant Cl_l ions at 3.026 \AA . The angles formed are $\text{Cl}_s\text{-Cu-N}$, 89.6° ; $\text{Cl}_l\text{-Cu-N}$, 90.4° ; and $\text{Cl}_s\text{-Cu-Cl}_l$ [i. e., $\text{Cl}(\text{I})\text{-Cu-Cl}(\text{I}')$ in the bottom drawing], 91.52° . Closest distances between carbon atoms on different rings are 3.759 \AA between pyridine (A) and pyridine (B) and 3.837 \AA between pyridine (A) and pyridine (B'); those between chlorine and carbon atoms are 3.687 \AA between $\text{Cl}(\text{I})$ and pyridine (A) and 3.785 \AA between $\text{Cl}(\text{II})$ and pyridine (A). Exchange paths of the type J_1' [$\text{Cu-Cl}(\text{I})\text{-pyridine (A)-Cu}$], J_2' [$\text{Cu-Cl}(\text{I}')\text{-pyridine (A')-Cu}$, shown on the bottom figure only] and J_2 [in direction b , along $\text{Cu-pyridine (C)-Cl}(\text{III})\text{-Cu}$, shown on top figure only] are indicated. Other contacts of interest include the closest $\text{Cl}(\text{I})$ to pyridine (A') separation of 4.942 \AA and the intrachain pyridine (A') to $\text{Cl}(\text{II})$ separations of 3.474 and 3.640 \AA .

\AA and two nitrogen atoms at 2.004 \AA and two more distant Cl_l ions at 3.026 \AA . The closest contact separations between chains (Fig. 1) involve 3.759-, 3.837-, 3.851-, and 3.965- \AA carbon-carbon separations and 3.687-, 3.785-, and 3.890 \AA carbon-chlorine separations. Of importance to our EPR resonance patterns (and g tensor) is the relative orientation of the two Cu-Cl_l separations, i. e., the angle between the Cu-Cl_l directions of inequivalent chains. This angle (47.60°) is two times the angle between the Cu-Cl_l direction and the a - c plane. The angle

formed by the projection of the Cu-Cl₁ direction onto the *a-c* plane and the *c* axis is 28.74°.

B. Nature of interchain coupling and relation to ordering temperature

The subtleties of the CPC structure are such that some discussion of the possible interchain interactions is required. Each Cu²⁺ ion is surrounded by eight neighboring Cu²⁺ ions on inequivalent chains at distances of 9.636 and 9.753 Å and by two Cu²⁺ ions on equivalent (simple lattice translation along *b*) chains at 8.560 Å. Although the nearest inequivalent neighbors form a slightly distorted body-centered structure, the superexchange paths are not all equal. As shown in Fig. 1, the body-centered copper (0, 0, 0) ion is coupled to those at the corners $\pm(\frac{1}{2}a, \frac{1}{2}b, \frac{1}{2}c)$ and $\pm(\frac{1}{2}a, -\frac{1}{2}b, \frac{1}{2}c)$ at 9.636 Å by a Cu-Cl₅-pyridine-Cu path [from Cl(I) to pyridine(A) in Fig. 1; the path pyridine(B) to Cl(II) is symmetry related] leading to an interaction J'_1 , whereas the coupling to those 9.753 Å away at the alternate four corners $\pm(\frac{1}{2}a, \frac{1}{2}b, -\frac{1}{2}c)$ and $\pm(-\frac{1}{2}a, \frac{1}{2}b, \frac{1}{2}c)$ of the cell are through a Cu-Cl₁-pyridine-Cu path [Cl(I') to pyridine(A') in Fig. 1] with an interaction J'_2 . The two nearest neighbors on equivalent chains at a distance 8.560 Å are also connected through paths of the type Cu-Cl₅-pyridine-Cu [from Cl(I) to pyridine(B')] and the interaction is J'_3 (note that there are two equivalent paths, i. e., Cl(I) to pyridine(B'); Cl(III) to pyridine(C) along *b*).

The path Cu-pyridine(A)-pyridine(B)-Cu = Cu-pyridine(A')-pyridine(B')-Cu, not involving Cl bonding at all, might also be considered as a possible source of superexchange, which would produce equal contributions to J'_1 and J'_2 .

In I it was pointed out that since the Cu-Cl₅ distance is 2.298 Å (using our current refined structure) and the Cu-Cl₁ distance is 3.026 Å, the strong interactions are likely to be J'_1 and J'_3 . The assumption $J'_1 = J'_3 \gg J'_2$ was made, which led to $Z' = 6$ neighbors and a Néel temperature which was asserted to be a function of $6J'_1$. This relation, however, is correct only for *ferromagnetic* order. In general the spin structure may be quite complicated, but as a simple example which illustrates the point, suppose that the ordered arrangement is as shown in Fig. 2, which would correspond to antiferromagnetic chains with the dominant interchain interaction being an antiferromagnetic J'_1 . Then if J'_2 and J'_3 are also antiferromagnetic, the net exchange field on the central ion will be $4(|J'_1| - |J'_2|) - 2|J'_3|$. The ordering temperature T_N is a function of this mean field. An effective interchain exchange constant may be defined by setting $Z'J'_{\text{eff}}$ equal to this mean field, where Z' interchain neighbors are taken into account. For the case of ten antiferromagnetically coupled neighbors in the lattice structure of Fig. 2, we find

$$J'_{\text{eff}} = \frac{2}{5}(|J'_1| - |J'_2|) - \frac{1}{5}|J'_3|,$$

while, if the assumption of I is made that $Z' = 6$ with $J'_1 = J'_3 \gg J'_2$, we obtain

$$J'_{\text{eff}} = \frac{1}{3}|J'_1|,$$

where J'_1 was termed *j* in I.

On the other hand, it will be shown in Sec. V that the effective exchange rate H_e between inequivalent chains as determined by the frequency-dependent linewidth gives a measure of $|J'_1 + J'_2|$, and is independent of J'_3 . Because of the very different dependences of H_e and of T_N on the interchain exchange constants, one cannot expect the two experiments (measurement of T_N and measurement of linewidth here) to yield the same value for a net effective interchain interaction J' , except in the unlikely event that $|J'_1| \gg |J'_2|, |J'_3|$.

III. EXPERIMENT

The linewidths were measured with standard microwave spectrometers. All linewidths reported are the peak-to-peak widths of the first derivative of the absorption spectrum. The *g* values and orientation of the principal axes of the *g* tensor were found to be in good agreement with I at Q band. The small blue needle-shaped crystals of CPC were grown following the methods described by Takeda *et al.*⁴ Crystals were checked by single-crystal photographic x-ray methods for twinning and strain; such imperfections were found to lead to somewhat broader lines at Q band at certain angles. The data reported are for strain-free crystals which were oriented by x-ray diffraction techniques.

IV. RESULTS

The crystal structure of CPC for magnetic purposes can be thought of as distorted octahedral

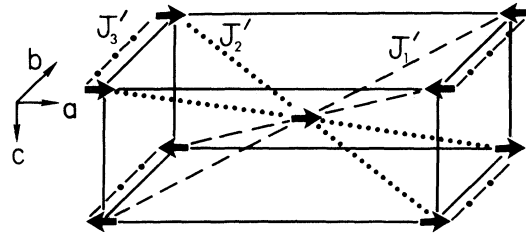


FIG. 2. Spin arrangement of antiferromagnetic chains expected in CPC below T_N if the dominant interchain interaction contributing to order is an antiferromagnetic J'_1 . Dashed lines show coupling J'_1 , dotted lines J'_2 , dash-dot lines J'_3 . See text and Fig. 1 for further explanation of the different interactions. Only the relative spin orientations should be considered. That is, the spins on the corners are expected to be parallel or antiparallel to the one in the center as shown, but we do not mean to imply that they lie in the *a* direction.

"molecules" of $\text{Cu}(\text{pyridine})_2\text{Cl}_4$ with the two Cl 's with the longest $\text{Cu}-\text{Cl}_l$ distances defining the axial tetragonal distortion from octahedral symmetry. All the molecules in one chain (parallel to the c axis) have the same orientation with the Cu 's strongly exchange coupled. Many Cu^{++} complexes of this kind have been studied,¹³ and it is found that the g tensor of the molecule is axially symmetric (in spite of the dissimilarity of the Cl 's and pyridines) with a \hat{g}_{\parallel} defined by the long $\text{Cu}-\text{Cl}_l$ direction and a \hat{g}_{\perp} perpendicular to the tetragonal distortion. In CPC there are magnetically inequivalent chains which are mirror images in the $a-c$ plane. Each \hat{g}_{\parallel} is tilted about 37° from the c axis as defined by the long $\text{Cu}-\text{Cl}_l$ bond, and the half-angle between the inequivalent \hat{g}_{\parallel} 's is 23.8° , as noted in Sec. II A. (The vector perpendicular to the plane is actually tilted about 38.5° from the c axis, not quite along $\text{Cu}-\text{Cl}_l$, due to the slight distortion of the copper environment; see angles in Fig. 1.) The crystal g tensor was analyzed in I and it was found that there was sufficient exchange between the chains so that resonances of the inequivalent chains could not be resolved at any angle with the X -band frequency employed. Thus the principal axes of the crystal g tensor were found to be determined by the average of the inequivalent chains, with the b axis being one of the three ($g_2 = 2.084$) and the other two (\hat{g}_1, \hat{g}_3) in the ac (mirror) plane; \hat{g}_1 is perpendicular to both \hat{g}_{\parallel} 's and is 62° from the c axis with a value of 2.061, which is a typical value for g_{\perp} ; \hat{g}_3 has the value 2.22 and is -28° from the c axis, in agreement with the value expected (28.74° , as in Sec. II A) if its direction bisects the two $\text{Cu}-\text{Cl}_l$ bonds in their plane. The measured principal values are consistent with a g_{\parallel} of 2.242 and a g_{\perp} of 2.061 for each of the inequivalent sites, with the angle between the two \hat{g}_{\parallel} axes perhaps a few degrees different from that between the $\text{Cu}-\text{Cl}_l$ long bonds, but only barely outside the limits of experimental accuracy of the g values and angular position of the crystal in the magnetic field. For the ensuing calculations we will assume that the two site \hat{g}_{\parallel} axes coincide with the $\text{Cu}-\text{Cl}_l$ directions and thus make an angle of 47.6° with respect to each other.

In order to determine the exchange rate between inequivalent chains, we have taken ESR spectra at 35 GHz, where the Larmor frequency is almost four times as great as in I. The signals of the individual sites still are not resolved at any angle, but the linewidth at selected angles is much greater at 35 GHz (Q band) than at 10.9 GHz (X band). All theories of exchange averaging predict that the frequency-dependent linewidth, due to inequivalent chains, lw , will go as the square of the splitting ΔH (in G) of the sites at a particular angle to the crystal:

$$lw = (\Delta H)^2 / H_e \quad (1a)$$

and thus the difference in total linewidths between Q and X band is

$$\Delta lw = \frac{(\Delta H_Q)^2 - (\Delta H_X)^2}{H_e} = \frac{9 \cdot 3(\Delta H_X)^2}{H_e}, \quad (1b)$$

where ΔH_X and ΔH_Q are the splittings at X band and at Q band, respectively. The quantity H_e depends on the rate of exchange between the equivalent sites. The linewidths in X band and Q band are plotted in Fig. 3 as a function of angle in the g_3 - b plane and the substantial difference is noted. Only one angle is really needed to determine H_e in Eq. (1b), but the full angular plot shows the dependence on the square of the splitting and the nearly-frequency-independent linewidths in symmetry directions. Because of the large intrachain interaction (280 GHz), the linewidths of the site resonances (with no inter-chain exchange) will have the same secular and non-secular dipolar values, and thus are not expected to be frequency dependent.

The splitting at any angle of the applied field to the crystal can be found by determining the angle between the field and each of the site \hat{g}_{\parallel} 's, which yields the g factor for each site and from the resonance condition (for Q band),

$$H = \frac{24\,971}{g} G,$$

the field position H of the resonance is obtained.

It is found that the maximum splitting occurs in a plane defined by the b axis and \hat{g}_3 (28.7° from c in the $a-c$ plane) which also contains the two site \hat{g}_{\parallel} axes. This splitting, to lowest order in $(g_{\parallel} - g_{\perp}) / (g_{\parallel} + g_{\perp})$, is given at 35 GHz by $\Delta H = 720 \sin 2\gamma$, in G, where γ is the angle between the field and the b axis in the g_3 - b plane. The solid curve in Fig. 3 results from using this value in Eq. (1b) together with $H_e = 6200$ G, to give a best fit at $\gamma = 45^\circ$. The angular dependence is seen to agree very well.

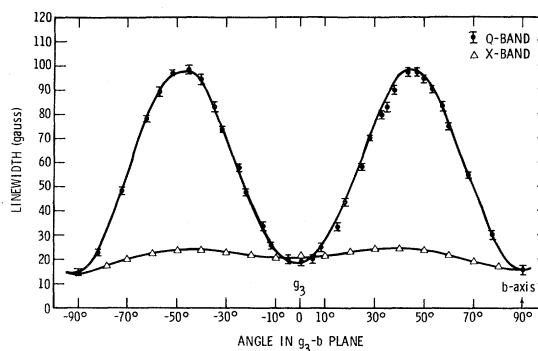


FIG. 3. Linewidth vs angle of applied field H when H is in the plane formed by the crystal b axis and the g_3 axis of the average g tensor, which is -28° from the c axis in the $a-c$ plane.

The crystal was tilted away from 45° in the $b\text{-}\hat{g}_3$ plane in all directions to make certain that the maximum linewidth was found, so that the main uncertainty in H_e comes from the uncertainty in the angle between the \hat{g}_i 's, where any error is magnified by the fact that the square of the splitting is used.

Data were also taken in the $b\text{-}c$ and $a\text{-}b$ planes with excellent agreement for the angular dependences. The maximum linewidths at X and Q band, respectively, were $b\text{-}c$ plane, 18 ± 1 and 75 ± 5 G; $a\text{-}b$ plane, 17 ± 1 and 50 ± 5 G. The large errors at Q band are due to the fact that the linewidths are a very strong function of angle for excursions out of the plane; a 5° deviation out of the $a\text{-}b$ plane gives a 10-G change in linewidth. To obtain agreement for the maxima in all the planes for one H_e , the site \hat{g} vectors were found to be a few degrees different from the Cu-Cl_1 direction, which leads to an uncertainty of $\pm 10\%$ in the value of H_e .

In the $a\text{-}c$ plane there should be no splitting because of symmetry, and it can be seen in Fig. 4 that the linewidths are independent of frequency within experimental error. The angular dependence of the linewidth can be understood from the angular dependence of the dipolar interaction.

It would be informative to take ESR spectra at a high enough frequency to actually resolve the two lines, so that the splitting (ΔH) is measured, rather than calculated from the behavior of site g factors in other Cu^{2+} complexes. However, even at the angle for maximum splitting it would require at least a 100-GHz Larmor frequency and even then the individual lines would be broadened to several hundred G by the large exchange rate and would be shifted towards the center by about $[\Delta H^2 - (H_e)^2]^{1/2}$.

Thus we would not expect a substantial improvement of the accuracy of the value of the exchange rate between chains by performing difficult high-frequency high-magnetic-field experiments, especially since so many Cu^{2+} complexes have been studied with fairly consistent results for the g tensors.

V. THEORY

It was stated in Eq. (1a) that the linewidth due to differing g tensors is given by $\Delta H^2/H_e$, where ΔH is the splitting which would be observed in the absence of coupling between the inequivalent chains and where H_e is an effective field which expresses the coupling. In this section we derive (1a) and give a formula for H_e terms of the inter- and intrachain exchange interactions. The model has two types of chains, A and B , with tensors \vec{g}_A and \vec{g}_B coupled by an interchain interaction J' which is much less than the intrachain interaction J . (For simplicity we refer to the interaction as J' when it is not necessary to distinguish between J'_1 and J'_2 of Fig. 2.) The chains are equivalent except for orientation of the

principal axes of the g tensors and thus J is the same for both chains. The Hamiltonian is then

$$\mathcal{H} = -2J \sum_{i_A} \vec{S}_{i_A} \cdot \vec{S}_{i_{A+1}} - 2J \sum_{i_B} \vec{S}_{i_B} \cdot \vec{S}_{i_{B+1}} - 2 \sum_{i_A, i_B} J'_{i_A, i_B} \vec{S}_{i_A} \cdot \vec{S}_{i_B} + \mu_B \vec{H} \cdot (\vec{g}_A \vec{S}_A + \vec{g}_B \vec{S}_B), \quad (2)$$

where the subscripts A and B refer to the different chain types, \vec{S}_A and \vec{S}_B are total spins of all the A - and B -type chains, respectively, μ_B is the Bohr magneton, and \vec{H} is the applied dc field. The separate broadening mechanism of intrachain dipolar coupling is neglected for the moment. The linewidth has been computed by Yokota and Koide¹⁴ for the situation in which the first two (intrachain) terms are absent from (2). In that case there is no 1d character to the problem and the exchange modulation is given by J' alone, with spin correlations decaying three-dimensionally. The basic ideas remain the same, however, when the intrachain terms are included, so that what immediately follows bears strong similarity to the development in Ref. 14.

For the case of interest here, observation of a single ESR line, the differing g tensors are treated as a perturbation which is modulated by J' . It is in the subsequent modulation of the interchain interaction by J that our work differs from Ref. 14. The final Zeeman term of Eq. (2) is written as

$$\mathcal{H}_z = \mathcal{H}_{z0} + \mathcal{H}'_z, \quad (3)$$

where

$$\mathcal{H}_{z0} = \mu_B \vec{H} \cdot \vec{g} \vec{S} = \mu_B \vec{S} \cdot \vec{g} \vec{H}, \quad (4)$$

$$\mathcal{H}'_z = \frac{1}{2} \mu_B \vec{H} \cdot \Delta \vec{g} \vec{H} = \frac{1}{2} \mu_B \vec{S} \cdot \Delta \vec{g} \vec{H}, \quad (5)$$

and where

$$\vec{S} = \vec{S}_A + \vec{S}_B, \quad (6)$$

$$\vec{S} = \vec{S}_A - \vec{S}_B, \quad (7)$$

$$\vec{g} = \frac{1}{2} (\vec{g}_A + \vec{g}_B), \quad (8)$$

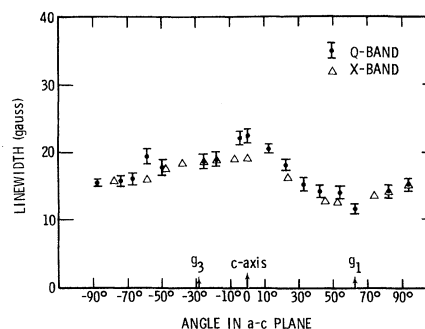


FIG. 4. Linewidth vs angle of applied field H when H is in the $a\text{-}c$ plane. Chains are magnetically equivalent in this case.

$$\Delta \vec{g} = (\vec{g}_A - \vec{g}_B). \quad (9)$$

The second equalities in (4) and (5) arise because \vec{g}_A and \vec{g}_B are symmetric tensors. The observed resonance frequency of the single line is

$$\omega = \mu_B |\vec{g} \vec{H}| / \hbar, \quad (10)$$

while the individual frequencies with which the A and B chains would resonate in the absence of J' are

$$\omega_{A,B} = \mu_B |\vec{g}_{A,B} \vec{H}| / \hbar. \quad (11)$$

The values of \vec{g}_A and \vec{g}_B are as given in Sec. IV.

The perturbation \mathcal{H}' is written as

$$\mathcal{H}' = \frac{1}{2} \mu_B s_{z'} (\Delta \vec{g} \vec{H})_{z'} + \frac{1}{2} \mu_B s_{\perp} (\Delta \vec{g} \vec{H})_{\perp}, \quad (12)$$

where z' is the axis of quantization defined by the direction of $\vec{g} \vec{H}$ and the subscript \perp indicates the component of $\Delta \vec{g} \vec{H}$ perpendicular to z' . The \perp term in (12) gives rise to nonsecular broadening¹⁴ which is negligible as long as $\omega t_c \gg 1$, where t_c is the correlation time for interchain spin diffusion. This condition is well satisfied here so that the second term in (12) is henceforth neglected. Since \vec{g}_A and \vec{g}_B have different symmetry axes, it is not in general true that

$$\mu_B (\Delta \vec{g} \vec{H})_{z'} = \hbar(\omega_A - \omega_B) \equiv \hbar \Delta \omega = g \mu_B \Delta H. \quad (13)$$

However, the relation is correct to lowest order in $\delta g/g$ [$\delta g \equiv g_{\parallel} - g_{\perp}$, $g \equiv \frac{1}{2}(g_{\parallel} + g_{\perp})$], and thus we can simplify (12) to

$$\mathcal{H}' = \frac{1}{2} \hbar \Delta \omega s_{z'}, \quad (14)$$

with the above-mentioned neglect of the nonsecular part.

The half-width in frequency units η is calculated from the Kubo-Tomita formula¹⁵

$$\eta = \int_0^{\infty} dt \frac{\langle G^{\dagger}(t)G(0) \rangle}{\langle M_x M_x \rangle} \quad (15)$$

in which

$$G(t) = \hbar^{-1} e^{i\mathcal{H}_0 t / \hbar} [\mathcal{H}', M_x] e^{-i\mathcal{H}_0 t / \hbar}, \quad (16)$$

where \mathcal{H}_0 is the exchange Hamiltonian [first three terms in Eq. (2)] and $M_{\pm} = M_x \pm M_y$. The exchange-narrowing formula Eq. (15) assumes that the integral converges, that the decay time of $G(t)$ is much less than $1/\eta$, and consequently that the line shape is Lorentzian. It is known⁹ that these conditions do not hold for a purely 1d system, so some question can arise as to the validity of (15) here. However, the time correlations to be studied are produced by J' and are thus 3d in character; hence we do not expect any of the 1d anomalies for that portion of the linewidth which is due to chains with different g tensors.

The expression for M_{\pm} in terms of the spin operators is complicated by the anisotropic and differ-

ent g tensors. But apart from corrections of the order of $\delta g/g$, we have simply

$$M_{\pm} = \mu g S_{\pm}, \quad (17)$$

which is adequate for our calculation to lowest order in δg since \mathcal{H}' is already proportional to δg . Use of (16) in (13)–(15) then gives

$$\eta = \frac{1}{4} \Delta \omega^2 \int_0^{\infty} \frac{\langle s^+(t) s^-(0) \rangle}{\langle s^+ s^- \rangle} dt \equiv \frac{1}{4} \Delta \omega^2 t_c, \quad (18a)$$

with $s^+(t) = e^{i\mathcal{H}_0 t / \hbar} s^+(0) e^{-i\mathcal{H}_0 t / \hbar}$, where we have noted that $\langle s^+ s^- \rangle = \langle s^+ s^- \rangle$, since there are no static interchain correlations, and have given formal definition to the correlation time t_c . Equation (18a) is essentially the same as found in Ref. 14.

Before proceeding we should note the comparison between Eq. (18a) and the expression

$$\eta = \frac{1}{8} \Delta \omega^2 t_c, \quad (18b)$$

derived¹⁶ for a model in which a spin jumps at random with a frequency $1/t_c$ between two sites where the frequencies differ by $\Delta \omega$. The factor-of-2 difference comes from evaluation of integrals of the type $|\int_0^t f(\tau) d\tau|^2$, where $f(\tau)$ is a random function. The form (18b) results if $f(\tau)$ can assume only two values, $\pm f_0$, say, whereas (18a) is appropriate if $f(\tau)$ can evolve continuously between $+f_0$ and $-f_0$. The correlation function $\langle s^+(t) s^-(0) \rangle$ has a continuous spectrum of values, and thus Eq. (18a)—which is used by other authors^{14,17} as well for exchange narrowing—seems to be the proper choice.

To evaluate $\langle s^+(t) s^-(0) \rangle$ we first observe that

$$\vec{S} = N^{1/2} \vec{S}_{\vec{Q}_0}, \quad (19)$$

where

$$\vec{S}_{\vec{Q}_0} = N^{-1/2} \sum_j \vec{S}_j e^{i\vec{Q}_0 \cdot \vec{r}_j}, \quad (20)$$

with N the total number of spins, is the wave-vector transform and where \vec{Q}_0 is a superlattice vector defined by

$$\vec{Q}_0 \cdot \vec{\delta} = \pi, \quad \vec{Q}_0 \cdot \vec{r}_A = 2n\pi, \quad (21)$$

in which we assume that each B site is related to an A site by $\vec{r}_B = \vec{r}_A + \vec{\delta}$. The CPC lattice shown in Fig. 1 essentially corresponds to such a picture with $\vec{\delta} = (\frac{1}{2}a, \frac{1}{2}b, \frac{1}{2}c)$.

Hence the problem reduces to calculating the zone-boundary wave-vector correlation $\langle S_{\vec{Q}_0}^+(t) S_{\vec{Q}_0}^-(0) \rangle$ which, for isotropic correlations, is equal to $2 \langle S_{\vec{Q}_0}^z(t) S_{\vec{Q}_0}^z(0) \rangle$. Hennessy *et al.*¹⁰ have treated $\langle S_{\vec{q}}^z(t) S_{\vec{q}}^z(0) \rangle$ in some detail for quasi-1d systems with finite interchain coupling. Their result is

$$\langle S_{\vec{Q}_0}^z(t) S_{\vec{Q}_0}^z(0) \rangle = \langle S_{\vec{Q}_0}^z S_{\vec{Q}_0}^z \rangle \exp \left[- \int_0^t (t - \tau) \tilde{\chi}_{\vec{Q}_0}(\tau) d\tau \right], \quad (22)$$

with

$$\tilde{\psi}_{Q_0}(\tau) = \frac{12\hbar^{-2}}{S(S+1)} N^{-1} \sum_q \langle \bar{S}_q^z(\tau) S_{-q}^z(0) \rangle^2 |J'_q - J'_{q-Q_0}|^2, \quad (23)$$

where the time dependence of $\bar{S}_q^z(\tau)$ is with respect to the dominant intrachain Hamiltonian only and where

$$J'_q = \sum_{jB} J'_{iAjB} e^{i\vec{q} \cdot \vec{r}_{iA} - i\vec{q} \cdot \vec{r}_{jB}}.$$

In (22) we have noted that $\bar{S}_{Q_0}^z(\tau) = S_{Q_0}^{z'}$, independent of τ , since \bar{S}_{Q_0} commutes with the intrachain exchange interaction [first two terms of Eq. (2)]. Reiter¹⁸ has pointed out that Eqs. (22) and (23) are derived from perturbation theory—with J' as the perturbation—and that a different form results in 1d if a self-consistent method is used. However, the correlation time t_c has the same dependence on J and J' in both Refs. 10 and 18, and the numerical approximations required in Ref. 18 in order to compute wave-vector sums make it questionable whether a more accurate expression for t_c has been obtained. We also note that an expression for t_c has recently been given in the literature which is identical to the one derived below.¹⁹

The quantity J'_q is given by

$$J'_q = 4(J'_1 + J'_2) \cos \frac{1}{2} q_1 a \cos \frac{1}{2} q_2 b \cos \frac{1}{2} q_3 c + 4(J'_2 - J'_1) \sin \frac{1}{2} q_1 a \cos \frac{1}{2} q_2 b \sin \frac{1}{2} q_3 c = -J'_{q-Q_0} \quad (24)$$

(q_1, q_2, q_3 are components along the crystal a, b, c axes, respectively) for the CPC lattice, considering only the nearest-neighbor A - B interchain couplings J'_1 and J'_2 , as shown in Fig. 1 and discussed in Sec. II B. Note that A - A and B - B interchain couplings (J'_3) play no immediate role in the relaxation since they commute with \bar{S}_{Q_0} . Upon converting the sum in (23) to an integral and using (24) we obtain

$$\tilde{\psi}_{Q_0}(\tau) = \frac{12\hbar^{-2}}{S(S+1)} \times 16 \frac{c}{\pi} \int_0^{\pi/c} dq_3 \langle \bar{S}_{q_3}^z(\tau) S_{-q_3}^z(0) \rangle^2 \times \left((J'_1 + J'_2)^2 \cos^2 \frac{q_3 c}{2} + (J'_1 - J'_2)^2 \sin^2 \frac{q_3 c}{2} \right) \quad (25)$$

by noting that $\langle \bar{S}_{q_3}^z(\tau) S_{-q_3}^z(0) \rangle$ depends only on q_3 .

From (22) and (25) it is evident that we are most interested in time development of $\tilde{\psi}_{Q_0}(\tau)$ for times such that $\frac{1}{2} \tilde{\psi}_{Q_0}(0) \tau^2 \sim 1$, which means for $S = \frac{1}{2}$, $\tau \sim (4J'/\hbar)^{-1}$. For $J' \ll J$ this time is very long compared with the characteristic decay time of $\tilde{\psi}_{Q_0}(\tau)$ itself, which is of the order of \hbar/J . Hence it is permissible to use the long-time diffusive expression

$$\langle \bar{S}_{q_3}^z(\tau) S_{-q_3}^z(0) \rangle^2 = \frac{1}{9} S^2 (S+1)^2 e^{-2Dq_3^2 \tau}, \quad (26)$$

where D is the diffusion coefficient, and to assume $D(\pi^2/c^2)\tau \gg 1$ so that the upper limit in (25) may be extended to ∞ , and the trigonometric functions in (25) replaced by their $q_3 = 0$ limits. We obtain

$$\tilde{\psi}_{Q_0}(\tau) = \frac{128}{3} \left(\frac{J'_1 + J'_2}{2} \right)^2 S(S+1) \pi^{-1/2} \left(\frac{2D\tau}{c^2} \right)^{-1/2} \quad (27)$$

and

$$\int_0^t (t-\tau) \tilde{\psi}_{Q_0}(\tau) d\tau = (t/t_1)^{3/2}, \quad (28)$$

where

$$t_1 = \left(\frac{9}{512 S(S+1)} \right)^{2/3} \left(\frac{2\pi D}{c^2} \right)^{1/3} (J'/\hbar)^{-4/3}, \quad (29)$$

in which $J' = \frac{1}{2}(J'_1 + J'_2)$ is the average interchain interaction. Note that $t_1 = 16^{-2/3} t_0$, where t_0 is the time defined in Ref. 10.

It follows from (18a), (22), and (29) that

$$t_c = t_1 \int_0^\infty e^{-x^{3/2}} dx = 0.9 t_1. \quad (30)$$

The diffusion coefficient for $S = \frac{1}{2}$ has been calculated²⁰ to be

$$D = \pi^{1/2} |J| c^2 / \hbar, \quad (31)$$

so that (29) and (30) reduce to

$$t_c = 0.16 \hbar \frac{|J|^{1/3}}{|J'|^{4/3}} \quad (32)$$

for spin $\frac{1}{2}$. Comparison of Eqs. (18a) and (1a) shows that

$$(g\mu_B/\hbar)H_e = 4t_c^{-1}(\frac{1}{2}\sqrt{3}), \quad (33)$$

where the factor $\frac{1}{2}\sqrt{3}$ is introduced to account for the relation between peak-to-peak separation and half-width for a Lorentzian line.

VI. ESTIMATE OF J' AND DISCUSSION

Our measured value of $H_e = 6200$ Oe when combined with the reported^{4,5} $|J|/k_B = 13.4$ °K yields

$$\frac{1}{2} |J'_1 + J'_2| = 0.16 \text{ °K} \equiv J'(t_c),$$

$$|J'(t_c)/J| = 1.2 \times 10^{-2},$$

where $J'(t_c)$ is a net effective J' as determined from the linewidth studies here. As discussed in Sec. II B, the effective exchange J'_{eff} may be inferred from the ordering temperature T_N . Values of $|J'_{\text{eff}}/J|$, inferred in I from T_N , ranged between 0.5×10^{-3} and 3.9×10^{-3} , depending on the theory used to relate T_N to the intrachain exchange J and the interchange exchange J'_{eff} . If, as in I, we assume $J'_1 = J'_3 \gg J'_2$, then we obtain $|J'_1/J| = 2.4 \times 10^{-2}$ from these linewidth studies, as compared to values ranging from 1.6×10^{-3} to 1.16×10^{-2} given by the T_N data. There is thus agreement to within about a factor of 2 for J'_1 in this picture, using the

Tahir-Kheli decoupling,²¹ which gives the largest J'_1 in terms of T_N . In view of the quantitative uncertainties of relative superexchange interactions and the theories of T_N and t_c , the agreement appears to be satisfactory. Even closer agreement could of course be obtained if J'_2 were non-negligible and $|J'_3| > |J'_1|$.

We further note that the larger $J'(t_c)$, rather than J'_{eff} , is the relevant interaction for eliminating the $e^{-t^{3/2}}$ line shape of a pure-1d system⁹; so the Lorentzian lines observed in I are readily explained by the magnitude of $J'(t_c)$ determined here, whereas it appeared in I, where J'_{eff} was used, that Lorentzian lines were only marginally consistent with the low ordering temperature $T_N = 1.13^\circ\text{K}$.

VII. SUMMARY AND CONCLUSIONS

We have used a novel technique to measure interchain exchange coupling in the quasi-one-dimensional salt CPC. The method, used here for the first time to our knowledge on a compound with chains of paramagnetic metal ions, is to study that part of the ESR linewidth which is caused by magnetically inequivalent chains. This contribution can be readily identified by its frequency and angular dependence. In the case of CPC the interchain coupling is sufficiently strong to merge the individual chain resonances into a single line whose width is given by Eqs. (1). The splitting in the absence of interaction, $\Delta\omega$, was deduced from the average g tensor measured in I together with site principal axes inferred from our refined crystal-structure determination. The fact that the Q-band angular dependence was in good agreement with the calculation confirms the assumed orientation of the site principal axes. The exchange field in (1), H_e , was related to the interchain interaction by the theory of Hennessy, McElwee, and Richards.¹⁰ The resulting interaction was such as to make $|J'(t_c)/J| = 1.2 \times 10^{-2}$, where $J'(t_c)$ is an effective value as measured in this experiment, assuming equal coupling to the eight nearest neighbors on inequivalent

chains. This ratio is at least a factor of 2 greater than a corresponding value $|J'_{\text{eff}}/J|$ inferred in I from the Néel temperature T_N . It was pointed out that since T_N is affected by the interaction between equivalent chains, J'_3 , whereas the frequency-dependent linewidth is not and that the two possible interactions between neighboring inequivalent chains, J'_1 and J'_2 , contribute to $J'(t_c)$ as $J'_1 + J'_2$ but contribute to J'_{eff} as $J'_1 - J'_2$, for antiferromagnetic chains, one cannot expect $J'(t_c)$ and J'_{eff} to be equal; and, in agreement with the results, the structure is such that $J'_{\text{eff}} < J'(t_c)$ for all antiferromagnetic interactions.

The frequency-dependent linewidth can provide an independent measurement of interchain coupling J' in compounds which have magnetically inequivalent chains. Unfortunately, it is not possible to use the method in CPC to make a detailed check of the relation between T_N and J' because the structure is too complex for a description in terms of only one interchain exchange constant. If a material can be found for which there is a single dominant interchain exchange, which is between magnetically inequivalent chains, then a truly meaningful verification of the theories of three-dimensional ordering in a quasi-one-dimensional system could perhaps be made. Such a study might also be possible with neutron scattering, but the small values of J' generally prevent the required determination of the magnon dispersion perpendicular to the chain axis.

A further advantage of studying the frequency-dependent part of the linewidth due to inequivalent chains is that one knows, from the g factors, just what the broadening mechanism is. This is particularly useful in non-S-state ions such as Cu^{2+} where the spin-spin broadening interaction may be appreciably nondipolar due to anisotropic exchange and where spin-lattice effects may influence the linewidth along symmetry directions. One cannot, of course, hope to obtain a quantitative value for the exchange interaction in a formula like Eqs. (1) unless the second-moment numerator is known.

†Work supported in part by the U. S. Atomic Energy Commission and by the National Science Foundation.

¹For reviews see D. Hone, AIP Conf. Proc. **5**, 413 (1971) and Ref. 2.

²D. Hone and P. M. Richards, Ann. Rev. Mater. Sci. **4**, 337 (1974); P. M. Richards, in *LIX Course of Enrico Fermi Summer School of Physics* (Academic, New York, to be published).

³This method has been used to define one-dimensionality in some organic charge-transfer (CT) complexes; see, for example, R. C. Hughes and Z. G. Soos, J. Chem. Phys. **48**, 1066 (1968), where J'/J for the CT salt *p*-phenylene diamine-chloranil was found to be $\sim 10^{-5}$.

⁴K. Takeda, S. Matsukawa, and T. Haseda, J. Phys. Soc. Jpn. **30**, 1330 (1971).

⁵W. Duffy, Jr., J. E. Venneman, D. L. Standburg, and

P. M. Richards, Phys. Rev. B **9**, 2220 (1974).

⁶Z. G. Soos, T. Z. Huang, J. S. Valentine, and R. C. Hughes, Phys. Rev. B **8**, 993 (1973).

⁷T. Z. Huang and Z. G. Soos, Phys. Rev. B **9**, 4981 (1974).

⁸T. Oguchi, Phys. Rev. **133**, A1098 (1964).

⁹R. E. Dietz, F. R. Merritt, R. Dingle, D. Hone, B. G. Silbernagel, and P. M. Richards, Phys. Rev. Lett. **26**, 1186 (1971).

¹⁰M. J. Hennessy, C. D. McElwee, and P. M. Richards, Phys. Rev. B **7**, 930 (1973).

¹¹J. Skalyo, Jr., G. Shirane, S. A. Friedberg, and H. Kobayashi, Phys. Rev. B **2**, 4632 (1970).

¹²J. D. Dunitz, Acta. Cryst. **10**, 307 (1957).

¹³C. J. Ballhausen, *Introduction to Ligand Field Theory* (McGraw-Hill, New York, 1962), p. 268.

¹⁴M. Yokota and S. Koide, J. Phys. Soc. Jpn. **9**, 953 (1954).

- ¹⁵R. Kubo and K. Tomita, *J. Phys. Soc. Jpn.* 9, 888 (1954).
- ¹⁶See, for example, A. Abragam, *Principles of Nuclear Magnetism* (Oxford U. P., New York, 1961); R. Kubo, in *Fluctuation, Relaxation and Resonance in Magnetic Systems*, edited by D. ter Haar (Plenum, New York, 1962).
- ¹⁷D. Kivelson, *J. Chem. Phys.* 27, 1087 (1957).
- ¹⁸G. Reiter, *Phys. Rev. B* 11, 5311 (1973).
- ¹⁹J. P. Boucher, F. Ferrieu, and M. Nechtschein, *Phys. Rev. B* 9, 3871 (1974). Although somewhat different approximations are used in Ref. 19 than in Ref. 10, the resulting values of t_c are identical for the special case of relaxation of \vec{S}_{Q_0} , since \vec{S}_{Q_0} commutes with the intrachain interaction.
- ²⁰R. A. Tahir-Kheli and D. G. McFadden, *Phys. Rev.* 182, 604 (1969).
- ²¹R. A. Tahir-Kheli, *Phys. Rev.* 132, 689 (1963); see also R. H. Swendson, *Phys. Rev. B* 5, 116 (1972).